



Endoplasmic Reticulum Stress Caused by Lipoprotein Accumulation Suppresses Immunity against Bacterial Pathogens and Contributes to Immunosenescence

Jogender Singh, Alejandro Aballay

Department of Molecular Genetics and Microbiology, Duke University Medical Center, Durham, North Carolina, USA

ABSTRACT The unfolded protein response (UPR) is a stress response pathway that is activated upon increased unfolded and/or misfolded proteins in the endoplasmic reticulum (ER), and enhanced ER stress response prolongs life span and improves immunity. However, the mechanism by which ER stress affects immunity remains poorly understood. Using the nematode *Caenorhabditis elegans*, we show that mutations in the lipoproteins vitellogenins, which are homologs of human apolipoprotein B-100, resulted in upregulation of the UPR. Lipoprotein accumulation in the intestine adversely affects the immune response and the life span of the organism, suggesting that it could be a contributing factor to immunosenescence. We show that lipoprotein accumulation inhibited the expression of several immune genes encoding proteins secreted by the intestinal cells in an IRE-1-independent manner. Our studies provide a mechanistic explanation for adverse effects caused by protein aggregation and ER stress on immunity and highlight the role of an IRE-1-independent pathway in the suppression of the expression of genes encoding secreted proteins.

IMPORTANCE Increased accumulation of unfolded and/or misfolded proteins in the endoplasmic reticulum (ER) leads to enhanced ER stress. However, the mechanism(s) by which ER stress affects immunity remain understudied. Using the nematode *C. elegans*, we showed that mutations in lipoproteins lead to their accumulation in the intestine, causing ER stress and adversely affecting the life span of the organisms and their resistance to pathogen infection. Our results indicate that the ER stress caused by lipoprotein accumulation significantly reduced the levels of expression of genes encoding secreted immune effectors, contributing to immunosenescence. It is known that ER stress may suppress gene expression via IRE-1, which is a sensor of ER stress. The novel mechanism uncovered in our study is IRE-1 independent, which highlights the role of a novel process by which ER stress suppresses innate immunity.

KEYWORDS *Caenorhabditis elegans*, ER stress, *Pseudomonas aeruginosa*, immune senescence, innate immunity, lipoproteins, unfolded protein response

The endoplasmic reticulum (ER) is a principal site where newly synthesized transmembrane and secretory proteins are folded, assembled, and undergo maturation. An increased accumulation of misfolded proteins in the ER can lead to ER stress (1). Indeed, a number of naturally occurring mutations detected in genetic diseases lead to aberrant protein folding, resulting in the ER stress observed in human diseases, including neurodegenerative diseases, diabetes, cancer, and inflammatory diseases (2–5). To cope with the ER stress, a series of unfolded protein response (UPR) pathways are activated. The UPR is an integrated intracellular signaling pathway that links the ER lumen to the cytoplasm and nucleus. Three parallel branches of the UPR—*ire-1*/*xbp-1*,

Received 9 May 2017 Accepted 11 May 2017 Published 30 May 2017

Citation Singh J, Aballay A. 2017. Endoplasmic reticulum stress caused by lipoprotein accumulation suppresses immunity against bacterial pathogens and contributes to immunosenescence. mBio 8:e00778-17. <https://doi.org/10.1128/mBio.00778-17>.

Editor Frederick M. Ausubel, Massachusetts General Hospital

Copyright © 2017 Singh and Aballay. This is an open-access article distributed under the terms of the [Creative Commons Attribution 4.0 International license](https://creativecommons.org/licenses/by/4.0/).

Address correspondence to Alejandro Aballay, a.aballay@duke.edu.

This article is a direct contribution from a Fellow of the American Academy of Microbiology. External solicited reviewers: Danielle Garsin, University of Texas Health Science Center at Houston; Ursula Jakob, University of Michigan–Ann Arbor.

atf-6, and *perk-1*—help to maintain ER homeostasis via a number of sophisticated mechanisms that control translation, protein degradation, mRNA degradation, and chaperone levels (6, 7). However, the UPR becomes compromised with age (8, 9), leading to enhanced protein aggregation in the ER.

Recent studies have shown that the UPR plays crucial roles in the regulation of the life span and immunity of organisms (9–11). Constitutive expression of the active form of XBP-1, that is part of the most conserved branch of the UPR, has been found to prolong life span (9). It has also been shown that bacterial infection causes damage to proteins at the site of infection, which leads to their aggregation (12), and that bacterial infection upregulates the UPR (13, 14). In addition, an increase in the UPR enhances the immunity of animals against bacterial infection (15–17).

We conducted a forward genetic screen in the nematode model organism, *Caenorhabditis elegans*, to identify dominant mutants exhibiting high UPR levels. We obtained several mutant animals with an upregulated UPR. Whole-genome sequencing (WGS) revealed that the UPR upregulation in these mutants resulted from mutations in vitellogenin proteins (VIT), which are lipoproteins involved in the transport of lipids from the intestine to oocytes and are homologs of human apolipoprotein B-100 (apoB-100). We show that mutations in lipoproteins result in their accumulation in the intestine, which causes ER stress and adversely affects the life span of the organisms and their resistance to pathogen infection. The upregulated UPR counteracts the toxic effects of ER stress and improves immunity and prolongs the life span of the mutants. Our studies also suggest that accumulation of lipoproteins may be a factor in immunosenescence. Quantification of the levels of expression of genes using RNA sequencing showed that ER stress caused by lipoprotein accumulation significantly reduced the expression levels of genes encoding secreted immune effectors. Our studies uncovered a novel mechanism by which ER stress suppresses innate immunity.

RESULTS

Forward genetic screen for mutants exhibiting UPR upregulation. We conducted a forward genetic screen using the UPR reporter strain SJ4005 *Phsp-4::gfp* to isolate mutants exhibiting an upregulated UPR (Fig. 1A). The transcription of *hsp-4*, the *C. elegans* ortholog of the mammalian ER-localized Hsp70 chaperone BiP, is upregulated in response to ER stress. An F₁ screen of approximately 80,000 ethyl methanesulfonate (EMS)-mutagenized haploid genomes resulted in the isolation of seven dominant mutants with enhanced green fluorescent protein (GFP) expression compared to the parental strain SJ4005 (see Fig. S1A in the supplemental material). All of the mutants showed very high levels of GFP in the intestine compared to the SJ4005 animals. We randomly selected five mutants for in-depth analysis (Fig. 1B). The enhanced GFP expression was completely blocked by knockdown of the UPR gene *xbp-1* and partially blocked by knockdown of the UPR gene *ire-1* by RNA interference (RNAi) (Fig. 1C and Fig. S1A). We confirmed activation of the UPR by monitoring the transcript levels of the ER chaperone genes *hsp-4* and *hsp-3* (Fig. 1D). The mutants had significantly higher levels of the ER chaperone transcripts than the SJ4005 animals did. However, the mutants did not show any significant changes in the transcript levels of *hsp-6* (Fig. S1B), a mitochondrial chaperone that is activated in the mitochondrial UPR. The mutants showed a slight but nonsignificant increase in the transcript levels of the cytosolic chaperone *hsp-16.2* (Fig. S1B), but these changes are marginal compared with those in *hsp-16.2* transcript levels upon heat stress (18), which induces *hsp-16.2*.

Interestingly, the mutants did not show enhanced GFP levels in comparison to SJ4005 animals until 62 h of growth at 20°C (Fig. 1E). The levels of GFP started to increase in the mutant animals only at 66 h, which coincides with the developmental stage at which L4 larvae molt into young adults. This finding indicated that the UPR was activated in the mutants only in the adult stage and not in the larval stages. Furthermore, the male mutant animals did not display any upregulation of the UPR compared to the SJ4005 animals (Fig. 1F). Taken together, these observations indicated that activation of the UPR in the mutant animals was specific to the adult hermaphrodites.

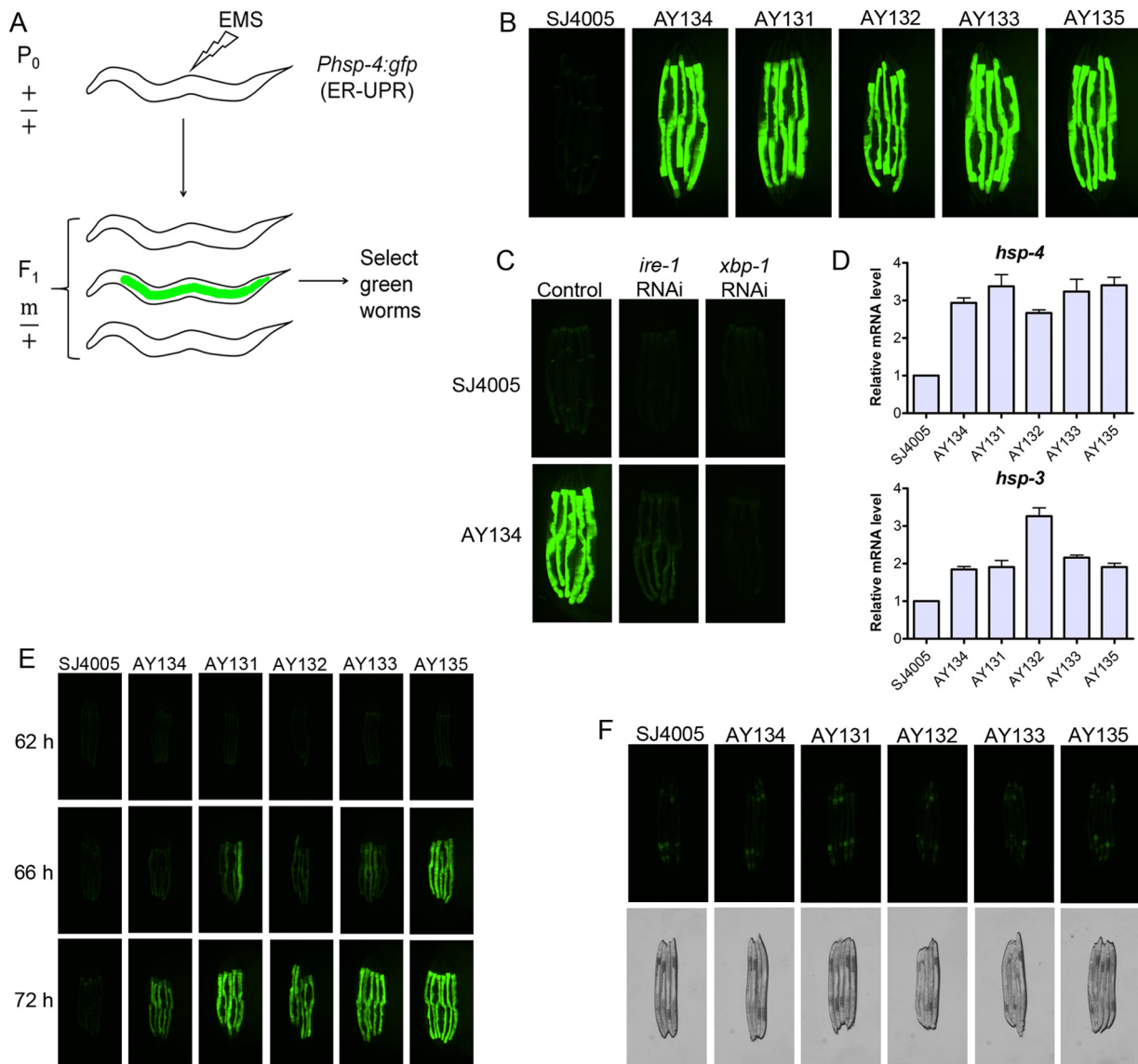


FIG 1 Forward genetic screen for mutants exhibiting an upregulated UPR. (A) Schematic for the forward genetic screen. The SJ4005 strain, which expresses *Phsp-4::gfp* and is a reporter strain for the ER UPR, was used for the screen. Mutants with high expression levels of GFP were screened from the F₁ progeny after mutagenesis. (B) Fluorescence images of five of the mutant animals and SJ4005 animals containing the reporter *Phsp-4::gfp*. The mutants isolated in the screen were designated AY131 to AY135. (C) Fluorescence images of one of the mutants and SJ4005 animals grown on empty RNAi vector or against the UPR genes *ire-1* and *xbp-1*. Animals grown on empty RNAi vector were used as the control. (D) Quantitative reverse transcription-PCR (qRT-PCR) for the ER chaperone genes *hsp-4* and *hsp-3* in the mutant and SJ4005 animals. The bar graphs show the means plus standard deviations (SD) (error bars) from three independent experiments. The *P* values for *hsp-4* RNA levels in mutant strains relative to SJ4005 animals are shown as follows: *P* < 0.001 for AY134, *P* < 0.001 for AY131, *P* < 0.01 for AY132, *P* < 0.001 for AY133, and *P* < 0.001 for AY135. The *P* values for *hsp-3* RNA levels in mutant strains relative to the levels in SJ4005 animals are as follows: *P* < 0.01 for AY134, *P* < 0.01 for AY131, *P* < 0.001 for AY132, *P* < 0.001 for AY133, and *P* < 0.001 for AY135. (E) Fluorescence images of the mutants and SJ4005 animals carrying the reporter *Phsp-4::gfp* during development at 20°C. The time represents the time of development from eggs at 20°C on *E. coli* OP50. Eggs represent the time point 0 h (F) Fluorescence images and the corresponding bright-field images of adult males of mutant and SJ4005 animals carrying the reporter *Phsp-4::gfp*.

Dominant mutations in vitellogenin/lipoprotein-encoding genes upregulate the UPR. To identify the causative mutations, we conducted whole-genome sequencing of the five selected mutants (Fig. 1B). The mutants were backcrossed six times with the parental strain SJ4005, and the sequenced genomes were aligned with the reference genome of *C. elegans*. After subtraction of the common variants, linkage maps of single nucleotide polymorphisms (SNPs) were obtained (Fig. S2). Analysis of the protein-coding genes carrying mutations in the mapped regions of each mutant revealed mutations in one of the six vitellogenin (*vit*) genes present in the *C. elegans*

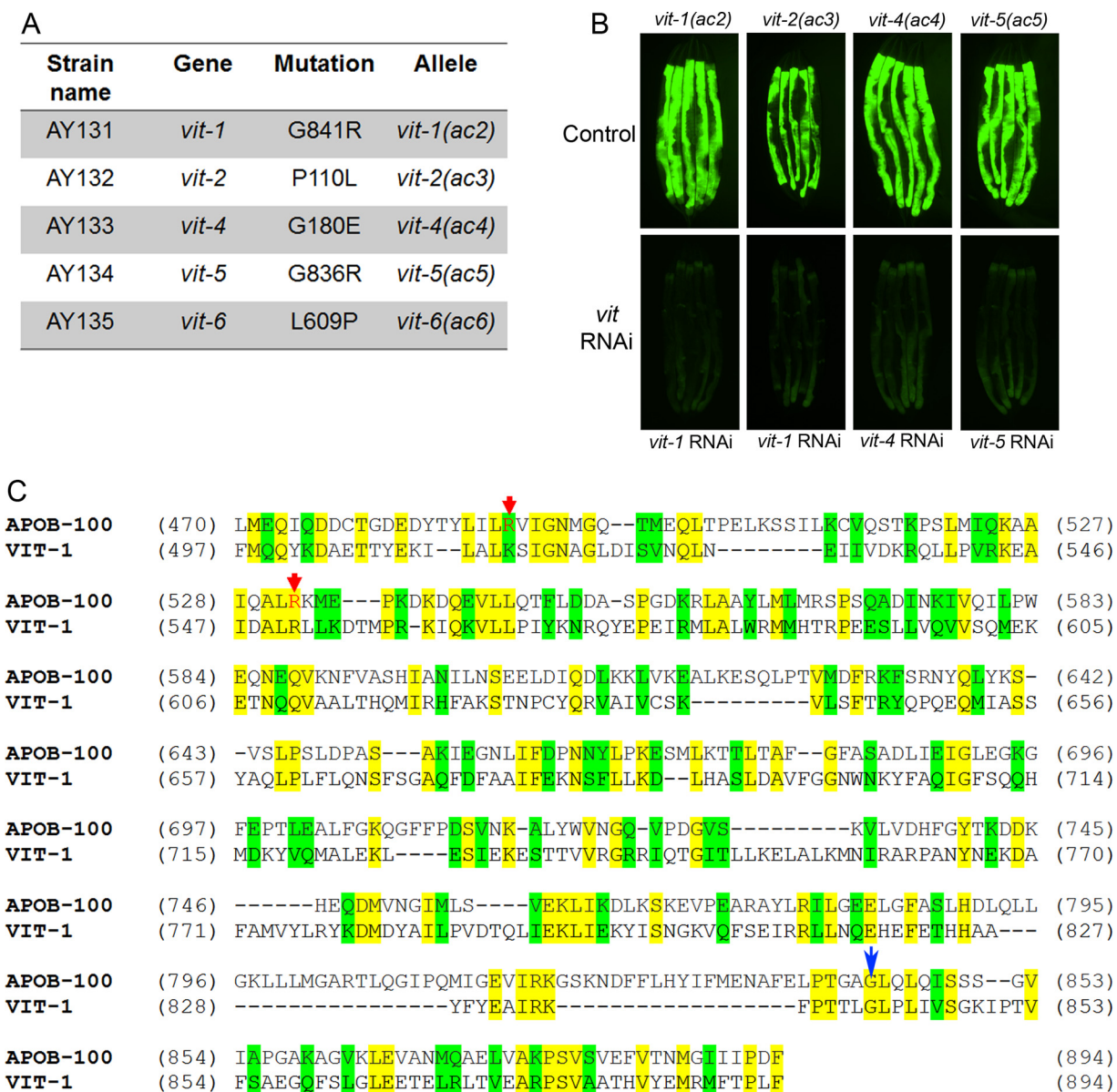


FIG 2 Mutations in vitellogenin genes activate the UPR in the mutants. (A) Table summarizing the mutations in the different *vit* genes identified by whole-genome sequencing in different UPR mutants. The corresponding amino acid changes in the VIT proteins are also shown. (B) Fluorescence images of the UPR mutants containing the reporter *Phsp-4::gfp* upon RNAi against *vit* genes. The control is empty vector control RNAi. (C) Sequence alignment of the conserved region of human apolipoprotein B-100 (APOB-100) with *C. elegans* VIT-1. Identical residues (yellow) and similar residues (green) are indicated. Red arrows point at residues whose mutations cause hampered secretion of apoB-100 and are linked with familial hypobetalipoproteinemia. The blue arrow highlights the conserved residue mutated in *vit-1(ac2)* and *vit-5(ac5)*.

genome (Fig. 2A). VIT proteins are lipoproteins that are expressed in the intestine of the adult hermaphrodite and are involved in the transport of lipids from the intestine to oocytes (19). Moreover, they have a high propensity to misfold and cause ER stress, and they are one of the most abundant proteins in *C. elegans* (20). This high abundance and propensity to cause ER stress may explain why all the mutations corresponded to *vit* genes.

Consistent with our results indicating that activation of the UPR was observed only in mutant hermaphrodites, *vit* genes are not expressed in males. Moreover, the UPR was upregulated in the mutants only in the intestine (Fig. 1B and Fig. S1A), the site of VIT protein synthesis. We reasoned that if upregulation of the UPR is caused by mutations in *vit* genes, inhibition of the mutated genes should rescue the phenotype. Among the genes encoding vitellogenins, a high level of sequence similarity is observed, resulting

in their classification into three groups. The *vit-1* and *vit-2* genes correspond to a group closely related to the group comprising *vit-3*, *vit-4*, and *vit-5*, while *vit-6* has a relatively low similarity to other *vit* genes (Fig. S3). The level of sequence similarity indicates that *vit-1* and *vit-2*, *vit-3*, *vit-4*, and *vit-5* would undergo complete cross RNAi (21). RNAi clones for *vit-2* and *vit-6* are unavailable in the two commercial *C. elegans* RNAi libraries, but given the aforementioned sequence similarity, RNAi against *vit-1* is expected to inhibit *vit-2*. Consistently, RNAi against *vit* genes caused a complete suppression of the enhanced UPR of the tested mutants (Fig. 2B).

Mutations in VIT proteins affect their transport and lead to accumulation in the intestine. Next, we sought to identify the mechanism by which the dominant mutations in *vit* genes activate the UPR. A previous study showed that reduction of unsaturated fatty acids in membranes upregulates the UPR in *C. elegans* (22). Because VIT proteins are involved in the transport of lipids, we decided to study whether the identified mutations may disturb lipid homeostasis in the intestine. To test whether the UPR upregulation was due to a reduction of unsaturated fatty acids, we supplemented the animal diets with different unsaturated fatty acids. Supplementation of the diet with fatty acids did not suppress the upregulated UPR (Fig. S4), indicating that the UPR was not upregulated due to a reduction of unsaturated fatty acids.

All of the mutations identified in the VIT proteins are nonconservative in nature. For example, in three isolated mutants, the smallest and neutral amino acid, glycine, is substituted by large and charged amino acids (Fig. 2A). These kinds of amino acid changes may lead to perturbations in the conformation of the protein, potentially resulting in aggregation. Two of the mutants also exhibited the same residue change, glycine for arginine, in a highly conserved region that is also present in human apoB-100 (23) (Fig. 2A and C). This conserved region of apoB-100 is known to have several disease-linked mutations (Fig. 2C), which promote misfolding and hampered secretion (24–26). VIT proteins are expressed in the intestine, from where they are secreted and transported to oocytes so that they can be incorporated into the developing embryos to provide nutrients (19). Thus, we tested whether the upregulated UPR observed in the isolated mutants might be caused by hampered secretion and subsequent accumulation of VIT proteins in the intestine. To examine this possibility, we generated transgenic animals expressing VIT-2::GFP and VIT-2(G839R)::GFP. VIT-2(G839R) carries a mutation analogous to the G841R and G836R mutations found in the *vit-1(ac2)* and *vit-5(ac5)* mutants.

Consistent with earlier studies (19), we observed VIT-2::GFP in both the intestine and embryo (Fig. 3A and Fig. S5). In contrast to VIT-2::GFP, VIT-2(G839R)::GFP remained in the intestine and was not transported to embryos (Fig. 3A). This finding indicated that the G839R mutation could lead to the misfolding and aggregation of VIT proteins, affecting secretion and transport to oocytes. Consistently, VIT-2(G839R)::GFP aggregates were observed in the intestine as well as in the pseudocoelomic region (Fig. 3B). Taken together, these data showed that activation of the UPR in the isolated mutants was caused by the accumulation of VIT proteins in the intestine.

Accumulation of VIT proteins leads to enhanced susceptibility to pathogens and a shortened life span. On the basis of the previous results, we hypothesized that the accumulation of VIT proteins might affect the intestinal immune response of all isolated mutants. Concomitant blockage of the ATF-6 and XBP-1 branches of the UPR and exposure to bacterial toxins are known to cause intestinal degeneration that results in smaller animals and paler intestines that are visible under the light microscope (13, 27). As shown in Fig. 4A, *vit-2(ac3)* animals exhibited smaller sizes and paler appearances compared to the parental strain SJ4005, and these morphological changes correlated with a strong susceptibility to infection by the pathogenic bacterium *Pseudomonas aeruginosa* PA14 (Fig. 4B and Table S1).

When the UPR was downregulated by RNAi against *ire-1*, *vit-2(ac3)* and *vit-6(ac6)* animals showed strong morphological changes associated with degeneration (Fig. 4C), while RNAi against *xbp-1* imposed those changes in all *vit* mutants (Fig. 4E). In contrast with the results shown in Fig. 4B, all of the mutants showed a strong susceptibility to

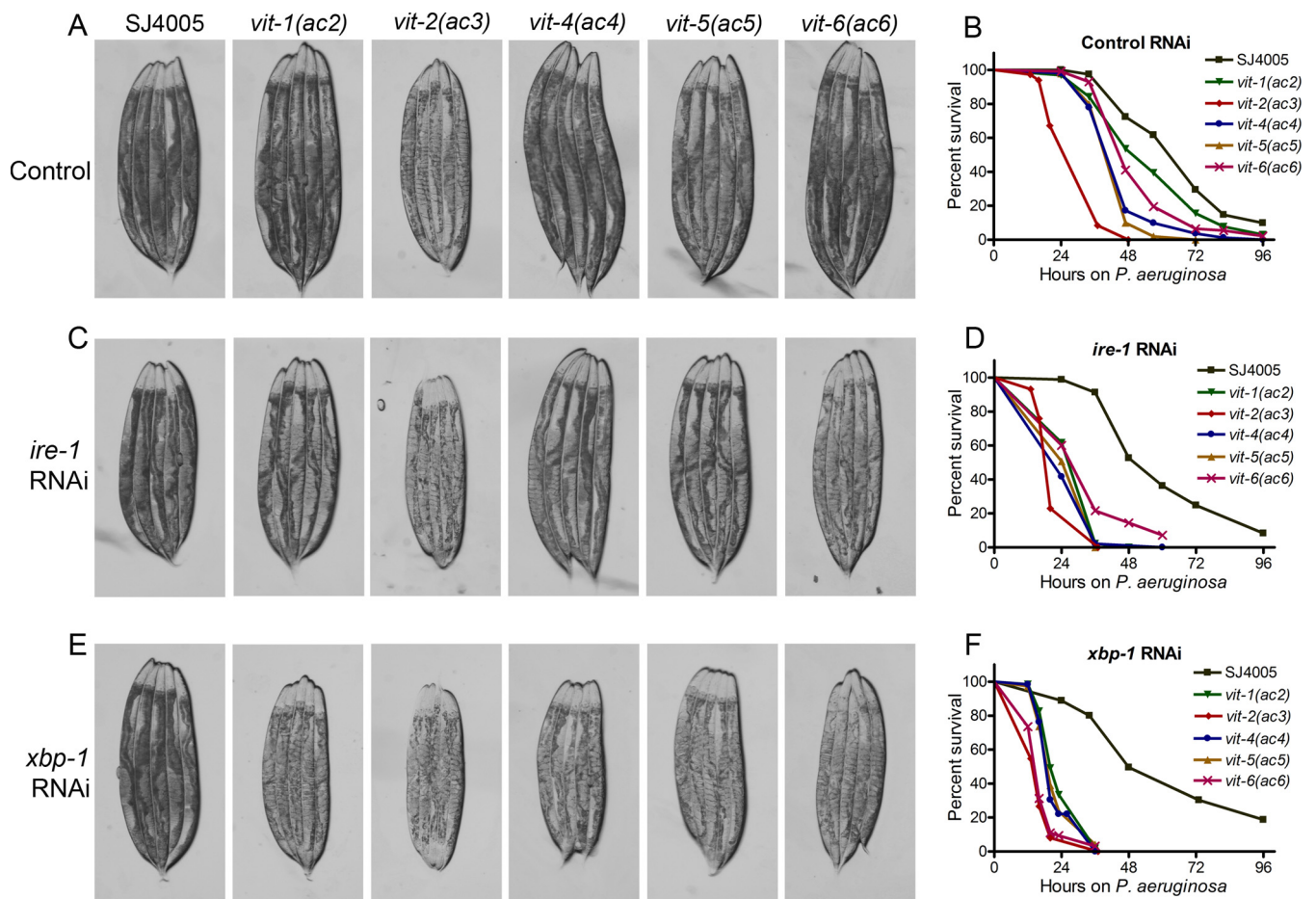


FIG 4 Accumulation of VIT proteins leads to intestinal degeneration. (A) Photomicrographs of the parental strain SJ4005 and mutant animals grown on *E. coli* HT115 containing empty vector at 20°C until they were 1-day-old adults before images were acquired. (B) Survival of SJ4005 and mutant animals on *P. aeruginosa* PA14 at 25°C after treatment with control RNAi. The animals were grown on *E. coli* HT115 containing empty vector at 20°C until they were 1-day-old adults before transferring to *P. aeruginosa* PA14 at 25°C. *P* values comparing the values for mutant animals to the values for SJ4005 animals are as follows: $P < 0.001$ for *vit-1(ac2)*, $P < 0.001$ for *vit-2(ac3)*, $P < 0.001$ for *vit-4(ac4)*, $P < 0.001$ for *vit-5(ac5)*, and $P < 0.001$ for *vit-6(ac6)*. (C) Photomicrographs of SJ4005 and mutant animals grown on *E. coli* HT115 containing vector for RNAi against *ire-1* at 20°C until they were 1-day-old adults before images were acquired. (D) Survival of SJ4005 and mutant animals on *P. aeruginosa* PA14 at 25°C after treatment with *ire-1* RNAi. The animals were grown on *E. coli* HT115 containing vector for RNAi against *ire-1* at 20°C until they were 1-day-old adults before being transferred to *P. aeruginosa* PA14 at 25°C. The *P* values for all mutant animals relative to the values for SJ4005 animals are $P < 0.001$. (E) Photomicrographs of SJ4005 and mutant animals grown on *E. coli* HT115 containing vector for RNAi against *xbp-1* at 20°C until they were 1-day-old adults before images were acquired. (F) Survival of SJ4005 and mutant animals on *P. aeruginosa* PA14 at 25°C after *xbp-1* RNAi. The animals were grown on *E. coli* HT115 containing vector for RNAi against *xbp-1* at 20°C until they were 1-day-old adults before being transferred to *P. aeruginosa* PA14 at 25°C. *P* values for all mutant animals relative to SJ4005 animals are $P < 0.001$. Survival curves are representative assays for three independent experiments. $n = 60$ to 100.

pathogen infection when RNAi against *ire-1* was used (Fig. 4D and Table S1). The susceptibility to pathogen infection was even stronger in mutants where *xbp-1* was inhibited by RNAi (comparison of Fig. 4D and F). Consistent with these results, *xbp-1* RNAi inhibited the observed UPR more efficiently than *ire-1* RNAi did (Fig. S1A).

There were no significant differences between the brood size of the mutants and that of SJ4005 animals (Fig. S6), suggesting that the accumulation in the intestine of a single VIT protein did not affect the overall transport of nutrients to oocytes. To

FIG 3 Legend (Continued)

animals. The red eclipse in the bottom panels are drawn around a single embryo. The yellow curved arrows indicate that the VIT-2 protein is transported to oocytes in VIT-2::GFP-expressing animals but not in VIT-2(G839R)::GFP-expressing animals. The images at the bottom of each column are a merge of the fluorescence and bright-field images. Bars, 100 μm . (B) VIT-2(G839R)::GFP-expressing animals showing the presence of GFP puncta in the intestine as well as the pseudocoelomic region; the VIT-2::GFP-expressing animals do not show any GFP puncta. The white arrows indicate GFP puncta. In all panels, the animals are young adults grown on *E. coli* OP50 at 20°C.

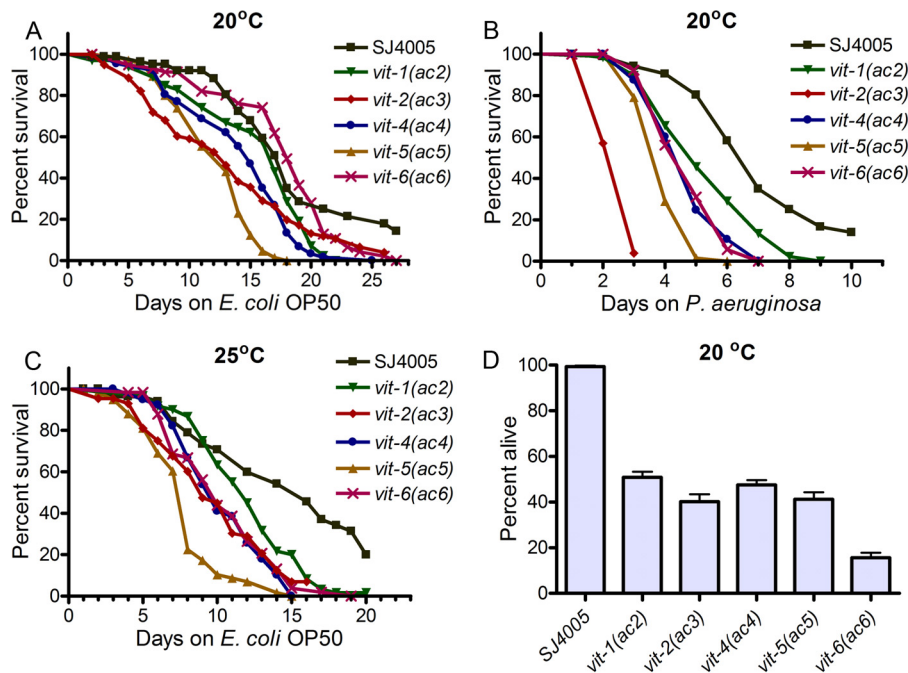


FIG 5 VIT protein accumulation adversely affects life span and enhances pathogen susceptibility. (A) Survival of SJ4005 and mutant animals on *E. coli* OP50 at 20°C. Day 0 represents young adults. *P* values for the values for mutant animals compared to the values for SJ4005 animals are as follows: $P > 0.05$ for *vit-1(ac2)*, $P < 0.001$ for *vit-2(ac3)*, $P > 0.05$ for *vit-4(ac4)*, $P < 0.001$ for *vit-5(ac5)*, and $P > 0.05$ for *vit-6(ac6)*. (B) Survival of SJ4005 and mutant animals on *P. aeruginosa* PA14 at 20°C. The animals were grown on *E. coli* OP50 at 20°C until they were 1-day-old adults before being transferred to *P. aeruginosa* PA14. *P* values comparing the values for mutant animals relative to the values for SJ4005 animals are as follows: $P < 0.01$ for *vit-1(ac2)*, $P < 0.001$ for *vit-2(ac3)*, $P < 0.001$ for *vit-4(ac4)*, $P < 0.001$ for *vit-5(ac5)*, and $P < 0.001$ for *vit-6(ac6)*. (C) Survival of SJ4005 and mutant animals on *E. coli* OP50 at 25°C. Day 0 represents young adults. *P* values comparing the values for mutant animals to the values for SJ4005 animals are as follows: $P < 0.05$ for *vit-1(ac2)*, $P < 0.001$ for *vit-2(ac3)*, $P < 0.001$ for *vit-4(ac4)*, $P < 0.001$ for *vit-5(ac5)*, and $P < 0.001$ for *vit-6(ac6)*. Survival curves are representative assays of three independent experiments. $n = 60$ to 100. (D) Percent of animals alive after 5 days of adult life span at 20°C after *xbp-1* RNAi. The bar graph shows the means plus SD from three independent experiments.

examine the effects of the mutations on the life spans of the animals, we compared the survival of the mutants with that of SJ4005 animals grown on nonpathogenic *Escherichia coli* OP50. While *vit-1(ac2)*, *vit-4(ac4)*, and *vit-6(ac6)* did not show any significant differences in life span, *vit-2(ac3)* and *vit-5(ac5)* had a significantly reduced life span at 20°C (Fig. 5A and Table S1). In contrast, all of the mutants showed significantly enhanced susceptibility to the pathogenic bacteria *P. aeruginosa* PA14 at 20°C (Fig. 5B and Table S1). These results indicated that while some mutants might have been able to survive as long as SJ4005 animals under nonstressed conditions, under the stress caused by infection, all of the mutants exhibited reduced survival compared to the SJ4005 animals. Consistent with the idea that an increase in temperature enhances proteotoxic stress (28), all of the mutants displayed reduced survival when grown on *E. coli* OP50 at 25°C (Fig. 5C and Table S1). The mutant animals also showed enhanced susceptibility to another pathogen, *Salmonella enterica* (Fig. S7).

The mutant animals exhibited a reduced life span upon *xbp-1* RNAi, and more than 50% of the mutant animals died within 5 days of adulthood (Fig. 5D). Taken together, these results show that the increased ER stress caused by accumulation of VIT proteins reduces the life span and enhances the pathogen susceptibility of animals, indicating that the upregulated UPR helped to alleviate the toxic effects of the ER stress on the animals. The results also indicate that the enhanced susceptibility of *vit-1(ac2)*, *vit-4(ac4)*, and *vit-6(ac6)* animals to pathogen infection at 20°C is not due to general sickness, suggesting that mutations in VIT proteins reduce immunity against bacterial infections.

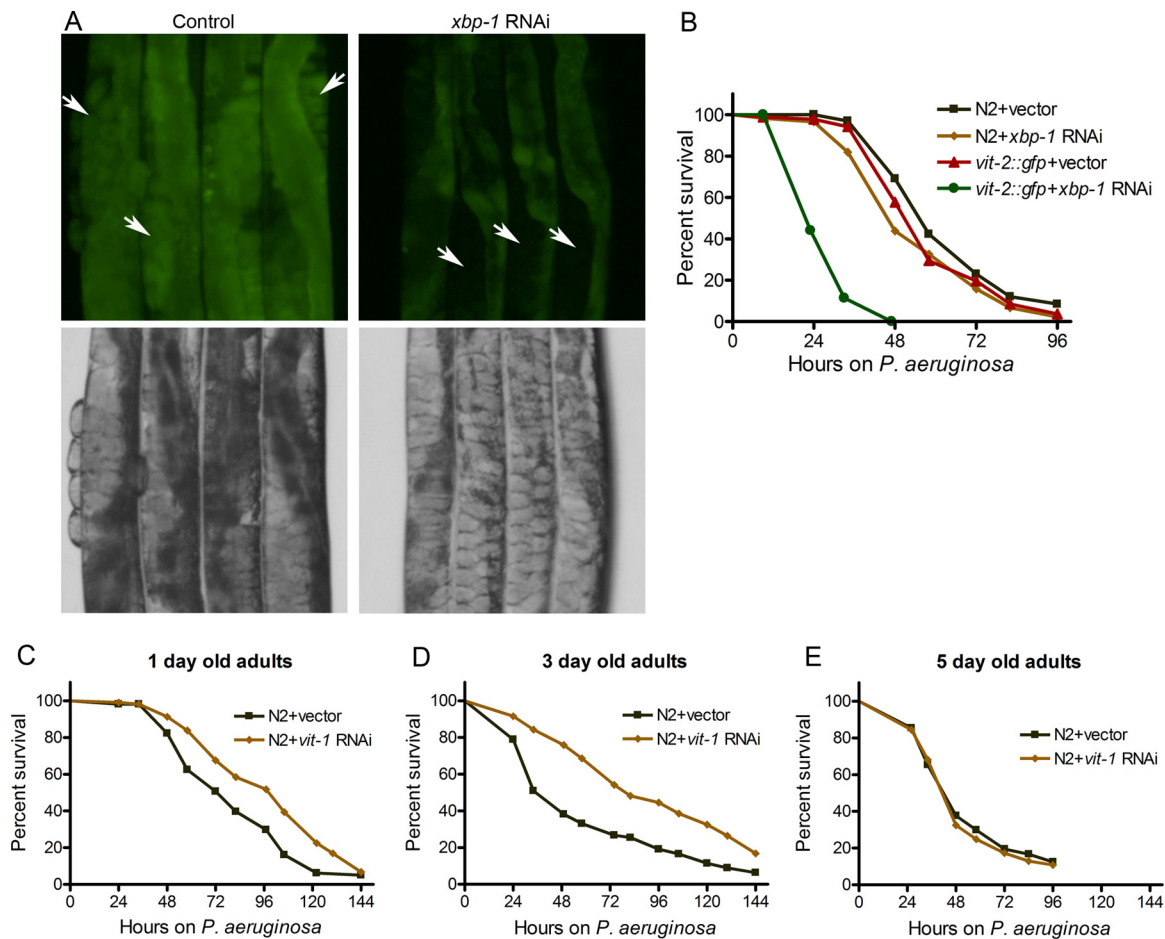


FIG 6 High levels of VIT proteins enhance susceptibility to pathogen infection. (A) Photomicrographs of 1-day-old adult transgenic animals expressing VIT-2::GFP with control and *xbp-1* RNAi. The white arrows point to embryos. (B) Survival of wild-type N2 animals and animals expressing VIT-2::GFP on *P. aeruginosa* PA14 at 25°C after treatment with control RNAi or *xbp-1* RNAi. The animals were grown on RNAi plates at 20°C until they were 1-day-old adults before being transferred to *P. aeruginosa* PA14 at 25°C. Comparing the value for control RNAi versus *xbp-1* RNAi for animals expressing VIT-2::GFP, $P < 0.001$. (C to E) Survival of N2 animals on *P. aeruginosa* PA14 at 25°C after treatment with control RNAi and *vit-1* RNAi. The animals were grown on RNAi plates at 20°C until they were 1-day-old, 3-day-old, and 5-day-old adults before being transferred to *P. aeruginosa* PA14 at 25°C.

High levels of VIT proteins enhance susceptibility to pathogen infection and contributes to immunosenescence.

It is known that the UPR decreases with aging (8, 9), with a concomitant increase in the levels of VIT proteins (29, 30). It is also known that the immune response decreases with aging (31, 32). To examine whether protein accumulation with aging may affect immunity, we decided to mimic some aspects of aging by blocking the UPR and by overexpressing VIT-2. While control RNAi animals displayed VIT-2::GFP mainly in the embryos, *xbp-1* RNAi animals primarily showed VIT-2::GFP in the intestine (Fig. 6A and Fig. S8). Consistent with our previous results indicating that VIT protein accumulation affects intestinal physiology, animals expressing VIT-2::GFP exhibited pale intestines upon *xbp-1* RNAi but not control RNAi (Fig. 6A and Fig. S8). As shown in Fig. 6B, *xbp-1* RNAi of animals expressing VIT-2::GFP had an enhanced susceptibility to *P. aeruginosa* infection compared to control RNAi. These results suggest that the accumulation of VIT protein in the intestine may negatively affect the response to infection. To address whether accumulation of VIT proteins with age affects the response to infection, we studied the pathogen susceptibility of aging animals upon knockdown of *vit* genes. We found that RNAi against *vit-1*, which is known to inhibit expression of other *vit* genes (30), enhanced the resistance to *P. aeruginosa* infection of 1-day-old adult animals (Fig. 6C). The resistance to *P. aeruginosa* infection upon *vit-1* RNAi was further enhanced in 3-day-old adult animals

(Fig. 6D). Aging *C. elegans* nematodes are known to have diminished UPR (9) and enhanced aggregation of the proteome (33, 34), and this overall proteotoxic stress correlates with enhanced susceptibility to pathogen infection (comparison of Fig. 6C to E). As shown in Fig. 6C and D, *vit-1* RNAi, which reduced the expression of one of the most abundant intestinal proteins, improved the resistance to *P. aeruginosa* infection of mildly aged *C. elegans*. However, *vit-1* RNAi had no effect on the resistance to *P. aeruginosa* infection in 5-day-old adult animals (Fig. 6E), suggesting that the deleterious effects of the overall misfolded proteome of 5-day-old animals cannot be reversed by only inhibiting VIT protein expression. Taken together, these results suggest that the accumulation of VIT proteins in the intestine may affect not only longevity but also immunity and that they may contribute to immunosenescence.

VIT accumulation leads to reduced gene expression of genes encoding secreted immune effectors. To understand the mechanism of enhanced susceptibility to pathogen infection caused by VIT accumulation, we used RNA sequencing to focus on transcriptional changes induced by VIT protein accumulation in *vit-2(ac3)* animals compared to SJ4005 animals. Of the 542 differentially regulated genes, 186 genes were upregulated, while 356 genes were downregulated (Table S2). Consistent with the idea that VIT protein accumulation induces ER stress, gene ontology analysis for biological function of the upregulated genes showed enrichment in genes linked to ER stress and the UPR (Table S2). Interestingly, we found that a subset of downregulated genes was enriched in ontology clusters associated with defense response, innate immune response, and defense responses to Gram-negative and Gram-positive bacteria (Table S2). These downregulated genes included lysozymes, saposin-like proteins (*spp* genes), and C-type lectins (Fig. 7A), which are conserved markers of immune activation that encode immune effectors secreted by the intestinal cells. For further analysis, we selected genes that have been experimentally linked to host defense against infections and confirmed their downregulation by quantitative reverse transcription-PCR (qRT-PCR) (Fig. 7B).

Because enhanced ER stress is known to activate regulated IRE-1-dependent degradation (RIDD) of mRNAs (35), we studied whether genes encoding secreted immune effectors were repressed by IRE-1. Thus, we compared the mRNA levels of immune genes of *vit-2(ac3) ire-1* RNAi animals to those of SJ4005 *ire-1* RNAi animals. We found that the expression level of 7 out of 8 immune genes was significantly inhibited in *vit-2(ac3)* animals in an IRE-1-independent manner (Fig. 7B). Thus, only a single studied gene, *thn-2*, showed partial IRE-1-dependent inhibition. These studies indicate that the expression of immune genes encoding secreted proteins is downregulated by the ER stress caused by accumulation of VIT proteins in an IRE-1-independent manner.

DISCUSSION

We demonstrated that mutations in lipoproteins in *C. elegans* led to their accumulation in the intestine and resulted in upregulation of the UPR. Although protein accumulation enhanced the UPR, which mitigated the adverse effects of accumulated VIT proteins on the isolated mutant animals, the animals exhibited enhanced susceptibility to pathogen infection and a shortened life span. Our results also indicate that the enhanced susceptibility to pathogen infection of animals exhibiting high ER stress due to accumulation of VIT proteins may be due to a mechanism activated by the resultant ER stress that inhibits the expression of a small subset of genes in the *C. elegans* genome that is highly enriched in immune effectors (Fig. 7C).

Surprisingly, even after cessation of the self-fertile reproductive period, the levels of VIT proteins continue to increase (29, 30, 36, 37). Moreover, not only does the amount of VIT proteins increase with age but also the rate of VIT protein synthesis increases (37). It is not clear why the VIT proteins are expressed even after cessation of the self-fertile reproductive period. One possibility is that VIT proteins remain necessary for reproduction by cross-fertilization, which occurs up to day 13 of adulthood (38) and is more than two times longer than the self-fertilization period. Another possibility is that the

A Immune-related genes downregulated in *vit-2(ac3)* compared to SJ4005

Gene name	Fold change (<i>vit-2(ac3)</i> vs SJ4005)	P-value
<i>thm-2</i>	-52.4	6.78E-07
<i>clec-209</i>	-32.3	2.44E-04
<i>ilys-5</i>	-26.3	3.96E-07
<i>spp-1</i>	-13.4	5.71E-06
<i>lys-8</i>	-10.7	5.35E-07
<i>lipl-5</i>	-9.2	1.59E-06
<i>spp-4</i>	-8.1	3.30E-04
<i>clec-186</i>	-7.4	3.82E-06
<i>clec-85</i>	-7.3	8.12E-05
ZK1320.2	-7.3	1.23E-05
<i>lys-7</i>	-6.5	6.52E-06
ZK228.4	-5.9	8.84E-06
F56F10.1	-5.2	5.77E-05
<i>spp-5</i>	-5.1	3.82E-05
F19C7.1	-4.9	5.75E-05
<i>clec-52</i>	-4.8	4.23E-04
K12H4.7	-4.5	2.60E-06
<i>spp-3</i>	-4.5	4.78E-05
<i>lys-1</i>	-4.5	1.26E-04
F35E12.6	-4.4	5.41E-04
<i>aqp-1</i>	-3.9	1.35E-04
<i>clec-187</i>	-3.3	4.02E-05
<i>grd-3</i>	-3.0	3.46E-04
<i>spp-2</i>	-2.8	5.05E-04
<i>maoc-1</i>	-2.7	1.49E-05
F31F7.1	-2.7	1.94E-04
F53C11.3	-2.4	5.90E-05
<i>clec-83</i>	-2.4	3.29E-04

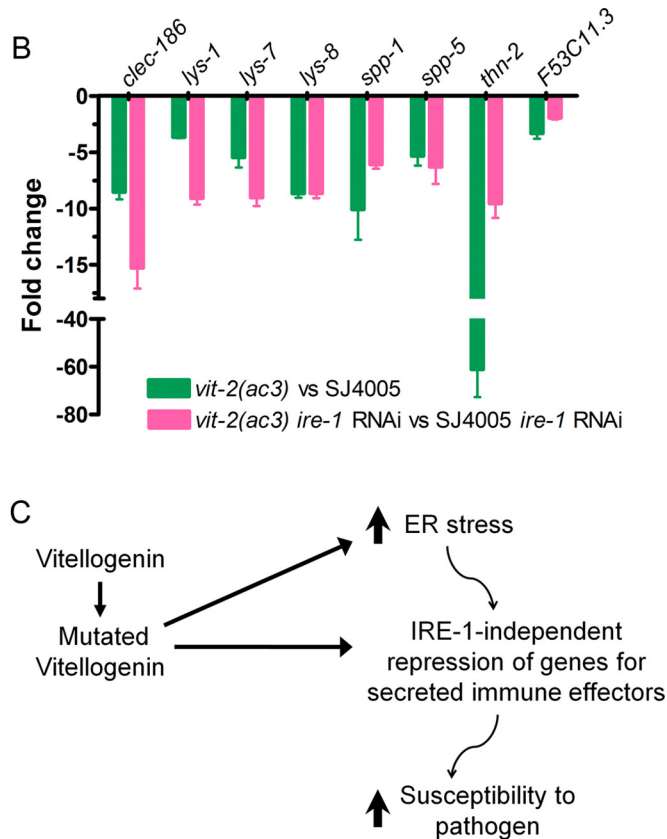


FIG 7 *vit-2(ac3)* animals exhibit reduced expression of immune genes. (A) List of immune-related genes that are downregulated in *vit-2(ac3)* animals compared to SJ4005 animals. (B) qRT-PCR for selected immune genes. The bar graph shows the means plus SD for three independent experiments. Comparing the values of all genes in *vit-2(ac3)* animals versus SJ4005 animals, $P < 0.0001$. (C) Model for the effects of mutations in vitellogenin proteins on innate immunity. Mutations in vitellogenin proteins lead to enhanced ER stress. Accumulation of mutated vitellogenin proteins and/or enhanced ER stress lead to suppression of secreted immune effectors in an IRE-1-independent manner, resulting in an enhanced susceptibility to pathogen infection.

animals are not under selection pressure after the reproductive period, and hence, no active mechanism has evolved to inhibit VIT protein expression during this period.

Gene expression and proteomic studies of several long-lived mutants have shown that these animals have reduced levels of *vit* genes and VIT proteins (30, 39–42). In addition, RNAi against different *vit* genes prolongs life span in multiple studies (30, 40, 43). Interestingly, long-lived mutants, which have reduced levels of *vit* genes and VIT proteins, carry mutations affecting different processes that are capable of controlling longevity, such as the *daf-2/daf-16* pathway, sterility, dietary restriction, and AMP-activated protein kinase pathway, among others. Even chemical substances such as garlic extract (44) and tyrosol (45), which enhance life span, lead to reduced levels of VIT proteins in animals. VIT proteins were also found to be highly abundant in insoluble fractions of the proteomes from aged animals (33, 34), likely because of their aggregation. Because all of the different longevity pathways seem to merge at reduced levels of VIT proteins, these studies highlight that one of the most downstream strategies utilized to enhance life span could be a reduction of the expression of aggregation-prone proteins such as lipoproteins. It has been shown that animals with a longer life span would also possess improved pathogen resistance (46). This could be due, at least in part, to reduced levels of aggregation-prone proteins, such as lipoproteins. Indeed, we observed that *vit-1* RNAi enhanced the resistance of animals to pathogens.

Several bacterial pathogens are known to induce ER stress in host cells. In *C. elegans*, both Gram-positive and Gram-negative pathogenic bacteria have been shown to enhance protein aggregation (12). These findings are further supported by the observation that pathogenic *P. aeruginosa* bacteria upregulate the UPR (14). Moreover,

P. aeruginosa infection led to reduced expression levels of genes *lys-7*, *spp-1*, and *thn-2*, which are required for optimal survival on *P. aeruginosa* (47). We found that these genes, which are also markers of immune activation by exposure to other pathogenic bacteria such as *Salmonella enterica* serovar Typhimurium and *Enterococcus faecalis*, were downregulated by the ER stress caused by VIT accumulation. Taken together, these results suggest that the ER stress caused by *P. aeruginosa* infection leads to downregulation of genes encoding secreted immune effectors.

In summary, our results provide evidence that the ER stress caused by protein accumulation results in the downregulation of genes encoding secreted proteins. Enhanced ER stress is known to lead to repression of specific mRNAs, which encode components of the plasma membrane and secreted proteins, by their degradation by IRE-1 (35). Here, we show that suppression of the immune genes encoding secreted proteins is independent of IRE-1. Our results also provide a mechanistic explanation for the adverse effects that high ER stress has on immunity. In future studies, it will be important to characterize the IRE-1-independent pathway(s) that may sense increased ER stress and elicit the suppression of genes encoding secreted proteins.

MATERIALS AND METHODS

Bacterial strains. The following bacterial strains were used: *Escherichia coli* OP50, *E. coli* HT115(DE3), *Pseudomonas aeruginosa* PA14, and *Salmonella enterica* serovar Typhimurium 1344. The cultures for these bacteria were grown in Luria-Bertani (LB) broth at 37°C.

***C. elegans* strains and growth conditions.** The *C. elegans* parental strain SJ4005 (*Phsp-4::gfp*) and wild-type Bristol N2 strains were obtained from the Caenorhabditis Genetics Center (University of Minnesota, Minneapolis, MN). The *C. elegans* strains were cultured under standard conditions and fed *E. coli* OP50.

Forward genetic screen for UPR upregulation. Ethyl methanesulfonate (EMS) mutagenesis was performed using the SJ4005 strain, which expresses green fluorescent protein (GFP) under the promoter of the *hsp-4* gene. Approximately 3,000 synchronized late L4 larvae of SJ4005 were treated with 50 mM EMS for 4 h and then washed three times with M9 medium. The washed animals (P0 generation) were then transferred to four large petri dishes (15 cm) containing *E. coli* OP50 and allowed to lay eggs of F₁ progeny overnight. The P0 animals were then washed away with M9 medium, while the F₁ eggs remained attached to the bacterial lawn. The F₁ eggs were allowed to grow to adulthood. The animals that showed enhanced GFP expression in the F₁ progeny were selected on individual plates. Approximately 80,000 haploid genomes were mutated in the screen. All of the mutants were backcrossed six times with the parental SJ4005 strain before analysis.

Fluorescence imaging. Animals were anesthetized using an M9 salt solution containing 30 mM sodium azide and mounted onto 2% agar pads. The animals were then visualized using a Leica M165 FC fluorescence stereomicroscope.

RNA interference. RNA interference (RNAi) was used to generate loss-of-function RNAi phenotypes by feeding nematodes *E. coli* strain HT115(DE3) expressing double-stranded RNA (dsRNA) homologous to a target gene (48, 49). Briefly, *E. coli* with the appropriate vectors were grown in LB broth containing ampicillin (100 µg/ml) and tetracycline (12.5 µg/ml) at 37°C overnight and plated onto NGM plates containing 100 µg/ml ampicillin and 3 mM isopropyl-β-D-thiogalactoside (IPTG) (RNAi plates). RNAi-expressing bacteria were allowed to grow overnight at 37°C. Gravid adults were transferred to RNAi-expressing bacterial lawns and allowed to lay eggs for 2 h. The gravid adults were removed, and the eggs were allowed to develop at 20°C to 1-day-old adults (96 h at 20°C from eggs) for subsequent assays. For age-dependent assays of N2 on *vit-1* RNAi, the eggs were allowed to reach 1-day-old adult stage on *vit-1* RNAi plates at 20°C (96 h at 20°C from eggs), 3-day-old adult stage (144 h at 20°C from eggs), and 5-day-old adult stage (192 h at 20°C from eggs) before transferring them to *P. aeruginosa* PA14 plates. *unc-22* RNAi was included as a positive control in all experiments to account for the RNAi efficiency. RNAi clones for *vit-2* and *vit-6* are unavailable in the libraries of J. Ahringer and M. Vidal. The rescue of the enhanced UPR in *vit-2(ac3)* was tested by *vit-1* RNAi thanks to cross-reactivity. The rescue of the enhanced UPR in *vit-6(ac6)* was not tested by RNAi due to the lack of cross-reactivity.

Whole-genome sequencing and data analysis. The mutant animals were grown at 20°C on NGM plates seeded with *E. coli* OP50 until starvation. The animals were rinsed off the plates with M9 medium, washed three times, incubated in M9 medium with rotation for 2 h to eliminate food from the intestine, and washed again three times with M9 medium. Genomic DNA extraction was performed using the Genra Puregene kit (Qiagen, Netherlands). DNA libraries were prepared according to a standard Illumina (San Diego, CA) protocol. The DNA was subjected to whole-genome sequencing (WGS) on an Illumina HiSeq 4000 sequencing platform using 50 single-end nucleotide reads. Library preparation and WGS were performed at the Duke Center for Genomic and Computational Biology.

The whole-genome sequence data were analyzed using the EMS density mapping workflow from the CloudMap program of the Galaxy web platform (50). The list of single nucleotide polymorphisms (SNPs) was generated by comparison to the reference genome WS220. Common SNPs were subtracted, and linkage maps were generated.

RNA isolation and quantitative reverse transcription-PCR. Animals were synchronized by egg laying. One hundred gravid adult animals were transferred to a 10-cm plate seeded with *E. coli* OP50 and allowed to lay eggs for 4 to 5 h. The gravid adults were then removed, and the eggs were allowed to develop at 20°C for 96 h. The animals were then collected, washed with M9 buffer, and frozen in TRIzol reagent (Life Technologies, Inc., Carlsbad, CA). Total RNA was extracted using the RNeasy Plus Universal kit (Qiagen, Netherlands). Residual genomic DNA was removed using TURBO DNase (Life Technologies, Inc., Carlsbad, CA). A total of 6 µg of total RNA was reverse transcribed with random primers using the High-Capacity cDNA reverse transcription kit (Applied Biosystems, Foster City, CA).

Quantitative reverse transcription-PCR (qRT-PCR) was conducted using the Applied Biosystems one-step real-time PCR protocol using SYBR green fluorescence (Applied Biosystems) on an Applied Biosystems 7900HT real-time PCR machine in 96-well plate format. Twenty-five-microliter reaction mixtures were analyzed as outlined by the manufacturer (Applied Biosystems). The relative fold changes of the transcripts were calculated using the comparative cycle threshold (C_T) ($2^{-\Delta\Delta C_T}$) method and normalized to pan-actin (*act-1*, *act-3*, and *act-4*). The cycle thresholds of the amplification were determined using StepOnePlus software (Applied Biosystems). All samples were run in triplicate. The primer sequences are available upon request.

RNA sequencing and data analysis. Total RNA samples for SJ4005 and *vit-2(ac3)* animals were isolated as described above. Three biological replicates were used to prepare RNA libraries using a Kappa standard mRNA sequencing kit. The RNA was sequenced on an Illumina HiSeq 4000 sequencing platform using 50 single-end nucleotide reads. Library preparation and sequencing were performed at the Duke Center for Genomic and Computational Biology.

The RNA sequence data were analyzed using Partek. Briefly, the RNA reads were aligned to the *C. elegans* genome (WS255) using the aligner STAR. Counts were normalized for sequencing depth and RNA composition across all samples. Differential gene expression analysis was then performed on normalized samples. Genes exhibiting at least twofold change and a false-discovery rate (FDR) of 1% or less were considered differentially expressed. Gene ontology analysis was performed using the DAVID Bioinformatics Database (david.abcc.ncifcrf.gov/).

Fatty acid supplementation assay. Fatty acid supplementation plates were made using an adapted protocol (51). Briefly, fresh 100 mM aqueous solution stocks of each supplement were made and added to NGM medium that had been cooled to 55°C to obtain a final concentration of 300 µM. The fatty acid salts were purchased from Sigma.

Generation of *C. elegans* transgenic lines. The plasmid V2B3, which encodes a functional VIT-2(YP170B)::GFP fusion protein expressed under the *vit-2* promoter, was a generous gift from Barth Grant (19). Site-directed mutagenesis was used to generate *vit-2(G839R)::gfp* plasmid. N2 wild-type animals were microinjected with *vit-2::gfp* plasmids along with pCFJ90 (*Pmyo-2::mCherry*) as a coinjection marker. The *vit-2::gfp* plasmids were used at a concentration of 25 ng/µl, while the coinjection marker was used at a concentration of 5 ng/µl. The plasmids were maintained as extrachromosomal arrays, and at least two independent lines were maintained for each plasmid.

Brood size assay. Five L4 animals were transferred to individual plates and incubated at 20°C. The animals were transferred to fresh plates every other day, and progeny were counted and removed every day.

***C. elegans* longevity assays.** Life span assays were performed on NGM plates containing *E. coli* OP50 or RNAi plates containing *E. coli* HT115(DE3) with the appropriate vector. Animals were scored as alive, dead, or gone every day. Animals that failed to display touch-provoked movement were scored as dead. Experimental groups contained 60 to 100 animals. The prefertile period of adulthood was used as $t = 0$ for the life span analysis. The assays were performed at 20 and 25°C.

***C. elegans* killing assays on *Pseudomonas aeruginosa* PA14.** The bacterial lawns used for *C. elegans* killing assays were prepared by spreading 20 µl of an overnight culture grown at 37°C of *P. aeruginosa* PA14 on the complete surface of modified NGM agar medium (0.35% peptone instead of 0.25% peptone) in 3.5-cm-diameter plates. The plates were incubated at 37°C for 12 to 16 h and then cooled to room temperature for at least 1 h before seeding with synchronized 1-day-old adult animals. The killing assays were performed either at 20°C or at 25°C as mentioned, and live animals were transferred daily to fresh plates. Animals were scored at the times indicated and were considered dead when they failed to respond to touch.

***C. elegans* killing assays on *Salmonella enterica*.** The bacterial lawns used for *C. elegans* killing assays were prepared by placing 20 µl of an overnight culture grown at 37°C of *S. enterica* on modified NGM agar medium (0.35% peptone instead of 0.25% peptone) in 3.5-cm-diameter plates. The plates were incubated at 37°C for 12 to 16 h and then cooled to room temperature for at least 1 h before seeding with synchronized 1-day-old adult animals. The killing assays were performed at 25°C, and live animals were transferred daily to fresh plates. Animals were scored at the times indicated and were considered dead when they failed to respond to touch.

SUPPLEMENTAL MATERIAL

Supplemental material for this article may be found at <https://doi.org/10.1128/mBio.00778-17>.

FIG S1, TIF file, 1.1 MB.

FIG S2, TIF file, 0.8 MB.

FIG S3, TIF file, 0.1 MB.

FIG S4, TIF file, 1.7 MB.

FIG S5, TIF file, 1 MB.

FIG S6, TIF file, 0.6 MB.

FIG S7, TIF file, 0.3 MB.

FIG S8, TIF file, 1 MB.

TABLE S1, XLSX file, 0.01 MB.

TABLE S2, XLSX file, 0.1 MB.

ACKNOWLEDGMENTS

Some strains were provided by the CGC, which is funded by the NIH Office of Research Infrastructure Programs (P40 OD010440). This work was supported by grants from the National Institutes of Health (GM0709077 and AI117911).

We thank Barth Grant (Rutgers University, Piscataway, NJ) for providing the *vit-2::gfp* plasmid.

We declare that we have no competing financial interests.

REFERENCES

- Shen X, Ellis RE, Lee K, Liu CY, Yang K, Solomon A, Yoshida H, Morimoto R, Kurnit DM, Mori K, Kaufman RJ. 2001. Complementary signaling pathways regulate the unfolded protein response and are required for *C. elegans* development. *Cell* 107:893–903. [https://doi.org/10.1016/S0092-8674\(01\)00612-2](https://doi.org/10.1016/S0092-8674(01)00612-2).
- Wang M, Kaufman RJ. 2016. Protein misfolding in the endoplasmic reticulum as a conduit to human disease. *Nature* 529:326–335. <https://doi.org/10.1038/nature17041>.
- Back SH, Kaufman RJ. 2012. Endoplasmic reticulum stress and type 2 diabetes. *Annu Rev Biochem* 81:767–793. <https://doi.org/10.1146/annurev-biochem-072909-095555>.
- Labbadia J, Morimoto RI. 2015. The biology of proteostasis in aging and disease. *Annu Rev Biochem* 84:435–464. <https://doi.org/10.1146/annurev-biochem-060614-033955>.
- Kaser A, Lee AH, Franke A, Glickman JN, Zeissig S, Tilg H, Nieuwenhuis EES, Higgins DE, Schreiber S, Glimcher LH, Blumberg RS. 2008. XBP1 links ER stress to intestinal inflammation and confers genetic risk for human inflammatory bowel disease. *Cell* 134:743–756. <https://doi.org/10.1016/j.cell.2008.07.021>.
- Ron D, Walter P. 2007. Signal integration in the endoplasmic reticulum unfolded protein response. *Nat Rev Mol Cell Biol* 8:519–529. <https://doi.org/10.1038/nrm2199>.
- Walter P, Ron D. 2011. The unfolded protein response: from stress pathway to homeostatic regulation. *Science* 334:1081–1086. <https://doi.org/10.1126/science.1209038>.
- Ben-Zvi A, Miller EA, Morimoto RI. 2009. Collapse of proteostasis represents an early molecular event in *Caenorhabditis elegans* aging. *Proc Natl Acad Sci U S A* 106:14914–14919. <https://doi.org/10.1073/pnas.0902882106>.
- Taylor RC, Dillin A. 2013. XBP-1 is a cell-nonautonomous regulator of stress resistance and longevity. *Cell* 153:1435–1447. <https://doi.org/10.1016/j.cell.2013.05.042>.
- Denzel MS, Storm NJ, Gutschmidt A, Baddi R, Hinze Y, Jarosch E, Sommer T, Hoppe T, Antebi A. 2014. Hexosamine pathway metabolites enhance protein quality control and prolong life. *Cell* 156:1167–1178. <https://doi.org/10.1016/j.cell.2014.01.061>.
- Janssens S, Pulendran B, Lambrecht BN. 2014. Emerging functions of the unfolded protein response in immunity. *Nat Immunol* 15:910–919. <https://doi.org/10.1038/ni.2991>.
- Mohri-Shiomi A, Garsin DA. 2008. Insulin signaling and the heat shock response modulate protein homeostasis in the *Caenorhabditis elegans* intestine during infection. *J Biol Chem* 283:194–201. <https://doi.org/10.1074/jbc.M707956200>.
- Bischof LJ, Kao CY, Los FCO, Gonzalez MR, Shen Z, Briggs SP, Van Der Goot FG, Aroian RV. 2008. Activation of the unfolded protein response is required for defenses against bacterial pore-forming toxin in vivo. *PLoS Pathog* 4:e1000176. <https://doi.org/10.1371/journal.ppat.1000176>.
- Richardson CE, Kooistra T, Kim DH. 2010. An essential role for XBP-1 in host protection against immune activation in *C. elegans*. *Nature* 463:1092–1095. <https://doi.org/10.1038/nature08762>.
- Dai L-L, Gao J-X, Zou C-G, Ma Y-C, Zhang K-Q. 2015. mir-233 modulates the unfolded protein response in *C. elegans* during *Pseudomonas aeruginosa* infection. *PLoS Pathog* 11:e1004606. <https://doi.org/10.1371/journal.ppat.1004606>.
- Sun J, Singh V, Kajino-Sakamoto R, Aballay A. 2011. Neuronal GPCR controls innate immunity by regulating noncanonical unfolded protein response genes. *Science* 332:729–732. <https://doi.org/10.1126/science.1203411>.
- Sun J, Liu Y, Aballay A. 2012. Organismal regulation of XBP-1-mediated unfolded protein response during development and immune activation. *EMBO Rep* 13:855–860. <https://doi.org/10.1038/embor.2012.100>.
- Douglas PM, Baird NA, Simic MS, Uhlein S, McCormick MA, Wolff SC, Kennedy BK, Dillin A. 2015. Heterotypic signals from neural HSF-1 separate thermotolerance from longevity. *Cell Rep* 12:1196–1204. <https://doi.org/10.1016/j.celrep.2015.07.026>.
- Grant BD, Hirsh D. 1999. Receptor-mediated endocytosis in the *Caenorhabditis elegans* oocyte. *Mol Biol Cell* 10:4311–4326. <https://doi.org/10.1091/mbc.10.12.4311>.
- Kimble J, Sharrock WJ. 1983. Tissue-specific synthesis of yolk proteins in *Caenorhabditis elegans*. *Dev Biol* 96:189–196. [https://doi.org/10.1016/0012-1606\(83\)90322-6](https://doi.org/10.1016/0012-1606(83)90322-6).
- Rual J-F, Klitgord N, Achaz G. 2007. Novel insights into RNAi off-target effects using *C. elegans* paralogs. *BMC Genomics* 8:106. <https://doi.org/10.1186/1471-2164-8-106>.
- Hou NS, Gutschmidt A, Choi DY, Pather K, Shi X, Watts JL, Hoppe T, Taubert S. 2014. Activation of the endoplasmic reticulum unfolded protein response by lipid disequilibrium without disturbed proteostasis in vivo. *Proc Natl Acad Sci U S A* 111:E2271–E2280. <https://doi.org/10.1073/pnas.1318262111>.
- Babin PJ, Bogerd J, Kooiman FP, Van Marrewijk WJ, Van der Horst DJ. 1999. Apolipoprotein II/I, apolipoprotein B, vitellogenin, and microsomal triglyceride transfer protein genes are derived from a common ancestor. *J Mol Evol* 49:150–160.
- Burnett JR, Shan J, Miskie BA, Whitfield AJ, Yuan J, Tran K, McKnight CJ, Hegele RA, Yao Z. 2003. A novel nontruncating APOB gene mutation, R463W, causes familial hypobetalipoproteinemia. *J Biol Chem* 278:13442–13452. <https://doi.org/10.1074/jbc.M300235200>.
- Zhong S, Magnolo AL, Sundaram M, Zhou H, Yao EF, Di Leo E, Loria P, Wang S, Bamji-Mirza M, Wang L, McKnight CJ, Figeys D, Wang Y, Tarugi P, Yao Z. 2010. Nonsynonymous mutations within APOB in human familial hypobetalipoproteinemia: evidence for feedback inhibition of lipogenesis and postendoplasmic reticulum degradation of apolipoprotein B. *J Biol Chem* 285:6453–6464. <https://doi.org/10.1074/jbc.M109.060467>.
- Yilmaz BS, Mungan NO, Di Leo E, Magnolo L, Artuso L, Bernardis I, Tumgor G, Kor D, Tarugi P. 2016. Homozygous familial hypobetalipoproteinemia: a Turkish case carrying a missense mutation in apolipoprotein B. *Clin Chim Acta* 452:185–190. <https://doi.org/10.1016/j.cca.2015.11.017>.
- Shen X, Ellis RE, Sakaki K, Kaufman RJ. 2005. Genetic interactions due to constitutive and inducible gene regulation mediated by the unfolded protein response in *C. elegans*. *PLoS Genet* 1:e37. <https://doi.org/10.1371/journal.pgen.0010037>.
- Vilchez D, Morante I, Liu Z, Douglas PM, Merkwirth C, Rodrigues APC, Manning G, Dillin A. 2012. RPN-6 determines *C. elegans* longevity under

- proteotoxic stress conditions. *Nature* 489:263–268. <https://doi.org/10.1038/nature11315>.
29. Herndon LA, Schmeissner PJ, Dudaronek JM, Brown PA, Listner KM, Sakano Y, Paupard MC, Hall DH, Driscoll M. 2002. Stochastic and genetic factors influence tissue-specific decline in ageing *C. elegans*. *Nature* 419:808–814. <https://doi.org/10.1038/nature01135>.
 30. Seah NE, de Magalhaes Filho CD, Petrashe AP, Henderson HR, Laguer J, Gonzalez J, Dillin A, Hansen M, Lapierre LR. 2016. Autophagy-mediated longevity is modulated by lipoprotein biogenesis. *Autophagy* 12: 261–272. <https://doi.org/10.1080/15548627.2015.1127464>.
 31. Shaw AC, Goldstein DR, Montgomery RR. 2013. Age-dependent dysregulation of innate immunity. *Nat Rev Immunol* 13:875–887. <https://doi.org/10.1038/nri3547>.
 32. Boraschi D, Aguado MT, Dutel C, Goronzy J, Louis J, Grubeck-Loebenstein B, Rappuoli R, Del Giudice G. 2013. The gracefully aging immune system. *Sci Transl Med* 5:185ps8. <https://doi.org/10.1126/scitranslmed.3005624>.
 33. David DC, Ollikainen N, Trinidad JC, Cary MP, Burlingame AL, Kenyon C. 2010. Widespread protein aggregation as an inherent part of aging in *C. elegans*. *PLoS Biol* 8:e1000450. <https://doi.org/10.1371/journal.pbio.1000450>.
 34. Reis-Rodrigues P, Czerwieńiec G, Peters TW, Evani US, Alavez S, Gaman EA, Vantipalli M, Mooney SD, Gibson BW, Lithgow GJ, Hughes RE. 2012. Proteomic analysis of age-dependent changes in protein solubility identifies genes that modulate lifespan. *Aging Cell* 11:120–127. <https://doi.org/10.1111/j.1474-9726.2011.00765.x>.
 35. Hollien J, Weissman JS. 2006. Decay of endoplasmic reticulum-localized mRNAs during the unfolded protein response. *Science* 313:104–107.
 36. Walther DM, Kasturi P, Zheng M, Pinkert S, Vecchi G, Ciryam P, Morimoto RI, Dobson CM, Vendruscolo M, Mann M, Hartl FU. 2015. Widespread proteome remodeling and aggregation in aging *C. elegans*. *Cell* 161: 919–932. <https://doi.org/10.1016/j.cell.2015.03.032>.
 37. Liang V, Ullrich M, Lam H, Chew YL, Banister S, Song X, Zaw T, Kassiou M, Götz J, Nicholas HR. 2014. Altered proteostasis in aging and heat shock response in *C. elegans* revealed by analysis of the global and de novo synthesized proteome. *Cell Mol Life Sci* 71:3339–3361. <https://doi.org/10.1007/s00018-014-1558-7>.
 38. Mendenhall AR, Wu D, Park SK, Cypser JR, Tedesco PM, Link CD, Phillips PC, Johnson TE. 2011. Genetic dissection of late-life fertility in *Caenorhabditis elegans*. *J Gerontol A Biol Sci Med Sci* 66:842–854.
 39. Halaschek-Wiener J, Khattra JS, McKay S, Pouzyrev A, Stott JM, Yang GS, Holt RA, Jones SJM, Marra MA, Brooks-Wilson AR, Riddle DL. 2005. Analysis of long-lived *C. elegans* daf-2 mutants using serial analysis of gene expression. *Genome Res* 15:603–615. <https://doi.org/10.1101/gr.3274805>.
 40. Murphy CT, McCarroll SA, Bargmann CI, Fraser A, Kamath RS, Ahringer J, Li H, Kenyon C. 2003. Genes that act downstream of DAF-16 to influence the lifespan of *Caenorhabditis elegans*. *Nature* 424:277–283. <https://doi.org/10.1038/nature01789>.
 41. Dong M-Q, Venable JD, Au N, Xu T, Park SK, Cociorva D, Johnson JR, Dillin A, Yates JR. 2007. Quantitative mass spectrometry identifies insulin signaling targets in *C. elegans*. *Science* 317:660–663. <https://doi.org/10.1126/science.1139952>.
 42. Burkewitz K, Morantte I, Weir HJM, Yeo R, Zhang Y, Huynh FK, Ilkayeva OR, Hirsche MD, Grant AR, Mair WB. 2015. Neuronal CRT-1 governs systemic mitochondrial metabolism and lifespan via a catecholamine signal. *Cell* 160:842–855. <https://doi.org/10.1016/j.cell.2015.02.004>.
 43. Yuan Y, Kadiyala CS, Ching TT, Hakimi P, Saha S, Xu H, Yuan C, Mullangi V, Wang L, Fivenson E, Hanson RW, Ewing R, Hsu AL, Miyagi M, Feng Z. 2012. Enhanced energy metabolism contributes to the extended life span of calorie-restricted *Caenorhabditis elegans*. *J Biol Chem* 287: 31414–31426. <https://doi.org/10.1074/jbc.M112.377275>.
 44. Huang CH, Hsu FY, Wu YH, Zhong L, Tseng MY, Kuo CJ, Hsu AL, Liang SS, Chiou SH. 2015. Analysis of lifespan-promoting effect of garlic extract by an integrated metabolite-proteomics approach. *J Nutr Biochem* 26: 808–817. <https://doi.org/10.1016/j.jnutbio.2015.02.010>.
 45. Cañuelo A, Peragón J. 2013. Proteomics analysis in *Caenorhabditis elegans* to elucidate the response induced by tyrosol, an olive phenol that stimulates longevity and stress resistance. *Proteomics* 13:3064–3075. <https://doi.org/10.1002/pmic.201200579>.
 46. Garsin DA, Villanueva JM, Begun J, Kim DH, Sifri CD, Calderwood SB, Ruvkun G, Ausubel FM. 2003. Long-lived *C. elegans* daf-2 mutants are resistant to bacterial pathogens. *Science* 300:1921.
 47. Evans EA, Kawli T, Tan M-W. 2008. *Pseudomonas aeruginosa* suppresses host immunity by activating the DAF-2 insulin-like signaling pathway in *Caenorhabditis elegans*. *PLoS Pathog* 4:e1000175. <https://doi.org/10.1371/journal.ppat.1000175>.
 48. Timmons L, Fire A. 1998. Specific interference by ingested dsRNA. *Nature* 395:854. <https://doi.org/10.1038/27579>.
 49. Fraser AG, Kamath RS, Zipperlen P, Martinez-Campos M, Sohrmann M, Ahringer J. 2000. Functional genomic analysis of *C. elegans* chromosome I by systematic RNA interference. *Nature* 408:325–330. <https://doi.org/10.1038/35042517>.
 50. Minevich G, Park DS, Blankenberg D, Poole RJ, Hobert O. 2012. CloudMap: a cloud-based pipeline for analysis of mutant genome sequences. *Genetics* 192:1249–1269. <https://doi.org/10.1534/genetics.112.144204>.
 51. Deline ML, Vrablik TL, Watts JL. 2013. Dietary supplementation of polyunsaturated fatty acids in *Caenorhabditis elegans*. *J Vis Exp* 81:e50879.